

A high acid mesoporous USY zeolite prepared by alumination

JINGHONG MA, YUHONG KANG, NING MA, WENMING HAO, YAN WANG, RUIFENG LI*

Key Laboratory of Coal Science and Technology, MOE, Institute of Special Chemicals, Taiyuan University of Technology, Taiyuan, 030024, China

A high-acidity HUSY zeolite with mesoporous structure was prepared by alumination with a dilute aqueous NaAlO_2 solution and characterized by XRD, N_2 adsorption, IR framework vibration and ^{29}Si MAS NMR methods. The results indicated the extra-framework aluminum was reinserted into the tetrahedral framework through isomorphic substitution of framework Si (0Al) sites by Al ions, whereas the crystal and micropore structure were unaltered. FTIR spectra of hydroxyl vibrations and pyridine adsorbed on realuminated zeolites showed that the number of Brønsted acid sites and strong Lewis acid sites increased whereas weak Lewis acid sites decreased twice. The mesoporous structure composed of inter- and intra-crystalline pores in the aluminated HUSY increased the external surface area of the zeolite, improving accessibility of molecules to the active sites and enhancing its catalytic ability. The realuminated HUSY zeolite supported with Ru catalyst exhibited a higher catalytic activity for benzene hydrogenation than the parent HUSY zeolite; the reaction rate in comparison to the meso-zeolite increased by 5.5 times.

Keywords: *meso-zeolite; alumination; HUSY; acid catalyst; catalytic hydrogenation*

© Wrocław University of Technology.

1. Introduction

The ultrastable Y (USY) zeolite, developed by dealumination of the crystal framework through the controlled addition of steam, is an active and key component of FCC (Fluid Catalytic Cracking) catalysts providing the major part of the surface area and active sites for catalytic cracking, isomerization and alkylation of hydrocarbons. The dealumination product HUSY exhibits high thermal and hydrothermal stability, hydrophobicity and catalytic activity in the petrochemical catalysis. Dealumination of zeolites leads to creation of a secondary pore system consisting of mesopores and extra-framework aluminum (EFAL) species. The removal of some Al atoms from the zeolite framework results in an increase of acidity and catalytic activity of the dealuminated zeolites, attributed to the interaction of bridging hydroxyls with extra framework Al–OH groups which are strong Lewis acid sites. At the same time, the hydrothermal dealumination of the zeolite framework slightly destroys the zeolitic crystal structure by the formation of mesopores. The presence of the mesopores reduces the diffusion paths of molecules in the microporous ze-

olite. Thereby the transport-limited reaction accelerates significantly, resulting in an improved catalyst effect [1]. On the other hand, EFAL species are responsible for the appearance of Lewis acidity; for low Si/Al zeolite Y, EFAL species have a promoting effect on the rates of isomerization, cracking, hydrogen transfer, and coking but increase the deactivating effect of coke. The influence of the Lewis acid sites on the protonic sites of the zeolite (“superacid sites”) is responsible for these effects [2–4].

For the majority of the acid-catalyzed reactions, the activity relates directly to the number of framework aluminum atoms, *i.e.* the number of Brønsted acid sites. It is obvious that the framework aluminum content must affect the population and the strength of these acid sites, which are responsible for the catalytic activity in many important reactions. The dealumination results in a loss of framework aluminum atoms, thus a decrease in the number of Brønsted active sites. Hence, it is desirable to reinsert aluminum into the dealuminated zeolite framework to improve Brønsted acid properties of the surface in the zeolite.

Several studies have been devoted to the post-synthetic incorporation of aluminum by adding another aluminum source externally in a synthesis system to obtain the zeolite with lower Si/Al ratio [5, 6].

*E-mail: rffi@tyut.edu.cn

The dealuminated zeolite was realuminated by the KOH treatment, whereby the extra-framework aluminum was re-inserted into the tetrahedral framework [7, 8]. It has been shown that the treatment of dealuminated zeolite Y with dilute aqueous solutions of bases (preferably KOH) yields samples with an enhanced content of framework aluminum; most of the extra-framework aluminum can be re-inserted. The treatment of the zeolite with a concentrated alkali aluminate solution (NaAlO_2) induced mild leaching of the framework silicon. The aluminations of zeolites by Al incorporation into the framework defects brings marked changes in the surface acidic properties of the solid, which are often coupled with their catalytic performance. However, the treatment of microporous zeolite (such as ZSM-5) with an aluminate solution of high alkalinity resulted in the samples whose porosity was mostly blocked by alkali ions deposits and silicate debris. The extraction step by acid washing had to be used to remove the Si-containing debris and NaAlO_2 -derived deposits from the alkali aluminate-treated zeolite [9].

In the present work, HUSY zeolite has been treated with a dilute aqueous NaAlO_2 solution to optimize its performance by realumination. The framework and pore structure of HUSY zeolites, before and after the treatment, were characterized by N_2 adsorption, XRD, FTIR spectroscopy and ^{29}Si MAS NMR; and their acidity was determined using FTIR spectra of hydroxyl groups and chemisorbed pyridine. The catalytic properties of HUSY zeolites before and after the treatment were investigated in benzene hydrogenation.

2. Experimental

2.1. Preparation of samples

HUSY zeolite sample was obtained by hydrothermal treatment of NH_4Y . The calcined HUSY sample was realuminated with the dilute NaAlO_2 aqueous solution. For example, 5 g HUSY zeolite was added into 300 ml NaAlO_2 aqueous solution with 0.01–0.1 mol/L concentration; the pH of solution was controlled below 13. The suspension was heated in a beaker at 80 °C for 6–24 h under stirring. The solid product was then separated by filtration,

washed and dried. The obtained samples were ion-exchanged triply with a 0.5 mol/g aqueous solution of NH_4NO_3 to yield NH_4 -form, and then calcined at 450 °C to obtain H-form samples. The resulting samples were denoted as HUSY-c-t, where c and t present the concentration of NaAlO_2 solution and time of treatment, respectively.

2.2. Characterization

X-ray diffraction (XRD) was recorded by Shimadzu D/Max-2500 diffractometer with $\text{CuK}\alpha$ X-ray source. The 2θ positions of the (111), (220), (311), (511), (440), (533), (642) peaks were used to calculate the average unit cell parameters, and the areas of (220), (311), (331), (511), (440), (533), (642) peaks were used to calculate crystallinity of the samples.

N_2 adsorption isotherms were obtained at -196 °C in a NOVA 1200e apparatus. BET surface area (S_{BET}) was calculated from the N_2 adsorption isotherm. The micropore volume (V_{micro}) and external surface area (S_{ext}) were determined using the t-plot method. The volume of mesopore (V_{meso}) was calculated using the BJH pore size model applied to the adsorption branch of the isotherm. Prior to this measurement, the samples were heated at 320 °C and evacuated for 4 h. FTIR spectra for the framework vibration, hydroxyl vibration and pyridine adsorbed on zeolite were recorded on Shimadzu 8400 using KBr wafer for the framework vibration, and the self-supporting wafer for hydroxyl vibration and adsorbed pyridine, respectively. The self-supporting wafer was mounted in a IR cell connected with an airtight system and activated under vacuum below 10^{-2} Pa at 673 K overnight. After the background spectrum (hydroxyl vibration) was collected, pyridine was introduced into the cell for 30 min at 150 °C until the saturated adsorption was reached. After the physisorbed pyridine was removed for 1 h at the same temperature, the IR spectrum was collected, and a stepwise desorption (at 150, 300, and 400 °C) was carried out to evaluate the strength of the acid sites.

^{29}Si MAS NMR spectra were obtained with the VARIAN UNITYINOVA 300M spectrometer at 59.584 MHz with 5 kHz spinning speed, 1.5 μs

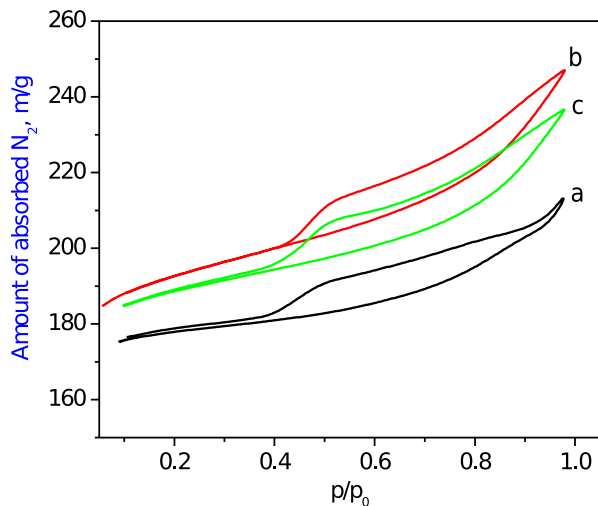


Fig. 1. N_2 adsorption/desorption isotherms of a) HUSY, b) HUSY-0.05-12 and c) HUSY-0.05-24.

excitation pulses and 3 s recycle time. Chemical shifts of silicon were referenced to tetramethylsilane (TMS).

The measurements of catalytic activities of Ru catalysts supported on HUSY in benzene hydrogenation reaction were performed in a 160 mL batch stirred reactor (Parr4842) at 40 °C and under 2.0 MPa pressure. Before reaction, 0.05 g of pre-reduced catalyst was transferred into the reactor in which 40 mL reactant had been introduced. The products were analyzed by a gas chromatograph (GC) equipped with a flame ionization detector (FID) and a column of polyglycol. Supported Ru catalysts were prepared by impregnating the zeolite with an aqueous solution of $RuCl_3$, and Ru content in all catalysts was 2.5 wt.%.

3. Results and discussion

3.1. Textural structure of HUSY zeolite treated by $NaAlO_2$

XRD patterns and IR spectra of framework vibrations of the HUSY zeolite samples were used to study the effect of $NaAlO_2$ treatment on the structure of zeolite. Compared with untreated HUSY zeolite, it can be seen that the samples treated with the $NaAlO_2$ solution retained the diffraction peaks corresponding to faujasite topology characteristic of

framework bonds. When the HUSY zeolites were treated with $NaAlO_2$ solution (at the concentration below 1.0 mol/L), the samples maintained their original crystallinity, but the lattice parameters increased, as shown in Table 1. Moreover, the frequency of IR band at $\sim 1050\text{ cm}^{-1}$, designed to an asymmetric stretch vibration ($\nu_{a(OTO)}$), was shifted to lower wavenumber. Both the increase in the unit cell parameter and the shift of $\nu_{a(OTO)}$ to lower wavenumber indicates that the Si/Al ratio in the zeolite framework has decreased.

In Fig. 1 the curves for nitrogen adsorption-desorption on HUSY zeolites before and after treatment with 0.05 mol/L $NaAlO_2$ solution are illustrated. A combination of type I and IV isotherms is observed for the parent HUSY sample. The existence of a hysteresis loop in the isotherms indicates the presence of mesopores. Upon alkaline treatment, the shape of the nitrogen adsorption and desorption is not significantly affected, suggesting the preservation of original microporous and mesoporous nature of HUSY zeolite. Moreover, the nitrogen isotherms of the treated zeolites show the enhanced uptake at relatively higher pressures and more distinct hysteresis loop, indicating the increase in the external surface area and mesopore volume as well as in the total surface area (Table 1).

The ^{29}Si NMR spectra of the HUSY samples untreated and treated with $NaAlO_2$ are shown in Fig. 2. Using Gaussian line shapes, five lines at around -90, -96, -102, -107, and -110 ppm, corresponding to Si(3Al), Si(2Al), Si(1Al), Si(0Al)_A, and Si(0Al)_B sites, were deconvoluted from the spectra of the HUSY samples, respectively. After treating with 0.05 mol/L $NaAlO_2$ solution, the distributions of these lines change obviously. As compared with the parent HUSY, the relative intensity of the lines at -96 and -102 ppm becomes more pronounced, while the intensity of lines at -107 and -110 ppm becomes weaker, showing the increase in the relative population of Si(2Al) and Si(1Al) sites, and decrease in Si(0Al) sites. Table 2 collects quantitative NMR results for the untreated and treated zeolites. It can be seen that the Si/Al ratio in the zeolite framework, calculated by deconvoluting NMR spectra, decreases from parent 6.33 to 5.06 and finally to 4.66 as the result of the treatment with $NaAlO_2$.

Table 1. Physical characteristics of HUSY zeolite.

Samples	Crystallinity [%]	u.c. parameter [Å]	$V_a(\text{OTO})$ [cm^{-1}]	S_{BET} [m^2/g]	V_{micro} [ml/g]	V_{meso} [ml/g]	S_{ext} [m^2/g]
HUSY	100	24.40	1057	522	0.26	0.07	40
HUSY-0.01-12	100	24.53	1054	570	0.26	0.10	71
HUSY-0.05-12	100	24.61	1048	591	0.26	0.11	91
HUSY-0.05-24	99	24.61	1046	559	0.26	0.10	70
HUSY-0.10-12	92	24.44	1044	518	0.23	0.09	67

Table 2. Quantification of untreated and treated zeolites with ^{29}Si MAS NMR.

Samples	Si(3Al)		Si(2Al)		Si(1Al)		Si(0Al) _A		Si(0Al) _B		Si/Al
	CS ^a	Area ^b	CS	Area	CS	Area	CS	Area	CS	Area	
HUSY	-89.7	2.00	-96.1	11.3	-102.1	34.4	-107.3	37.8	-109.3	14.4	6.3
HUSY-0.05-12	-89.2	2.55	-96.2	17.2	-102.1	37.0	-107.1	33.9	-109.1	9.35	5.1
HUSY-0.05-24	-90.0	1.27	-96.7	21.1	-102.4	39.7	-107.5	33.4	-111.6	4.45	4.7

^aChemical shift, ppm;

^bRelative area of peak, %.

The results of XRD, IR and NMR indicate that the HUSY zeolite has been realuminated during the treatment with NaAlO_2 solution. Furthermore, according to the experimental results of NMR, the relative population of $\text{Si}(\text{0Al})_{\text{A}}$ sites and $\text{Si}(\text{0Al})_{\text{B}}$ sites in the treated samples is lower than that in the parent zeolite, whereas the relative population of $\text{Si}(\text{1Al})$ and $\text{Si}(\text{2Al})$ sites in the treated samples is higher than that in the parent zeolite. It can be reasonably concluded that the realumination of HUSY in a dilute NaAlO_2 solution occurs through isomorphous substitution of Si atom by Al atom at $\text{Si}(\text{0Al})$ sites, thus generating new $\text{Si}(\text{1Al})$ and $\text{Si}(\text{2Al})$ sites in the framework of the HUSY zeolites.

3.2. Acidity of HUSY zeolites before and after realumination

Fig. 3 shows the FTIR spectra of a dehydrated HUSY zeolite before and after realumination in the spectral region of the stretching OH vibrations. Several distinct OH bands are observed, which are assigned to terminal silanol (3740 cm^{-1}), bridging $\text{Si}(\text{OH})\text{Al}$ in the supercages (3620 cm^{-1}) and the sodalite cages (3560 cm^{-1}), $\text{Si}(\text{OH})\text{Al}$ inside the supercages and the sodalite cages interacting with extra-framework aluminum (3600 and 3530 cm^{-1}), and Al–OH groups from extra-framework aluminum

Table 3. Quantification of B and L acid sites from pyridine-adsorbed IR spectra.

Samples	150 °C		300 °C		400 °C	
	B ^a	L ^b	B ^a	L ^b	B ^a	L ^b
HUSY	271	151	233	38	156	19
HUSY-0.05-12	313	82	274	47	217	36
HUSY-0.05-24	375	67	360	57	274	57

^aThe amount of Brønsted acid sites, $\mu\text{mol}/\text{g}$

^bThe amount of Lewis acid sites, $\mu\text{mol}/\text{g}$

species (3665 cm^{-1}), respectively [10]. Compared with the untreated HUSY, the bands at 3620 and 3560 cm^{-1} increased in intensity, showing that some supercages were renovated by the reinsertion of Al atoms in the sodalite cages of the zeolite. In addition, the hydroxyl spectra of the realuminated HUSY zeolite shows that the relative intensity of the bands at 3600 and 3530 cm^{-1} decreased as the relative intensity of the band at 3665 cm^{-1} of extra-framework aluminum species decreased.

The FTIR spectra of the pyridine adsorbed on HUSY samples before and after realumination show the bands at 1540 and 1450 cm^{-1} related to the adsorption of the pyridine molecules on Brønsted and Lewis acid sites. The quantitative results of the acid sites at pyridine desorption temperatures of

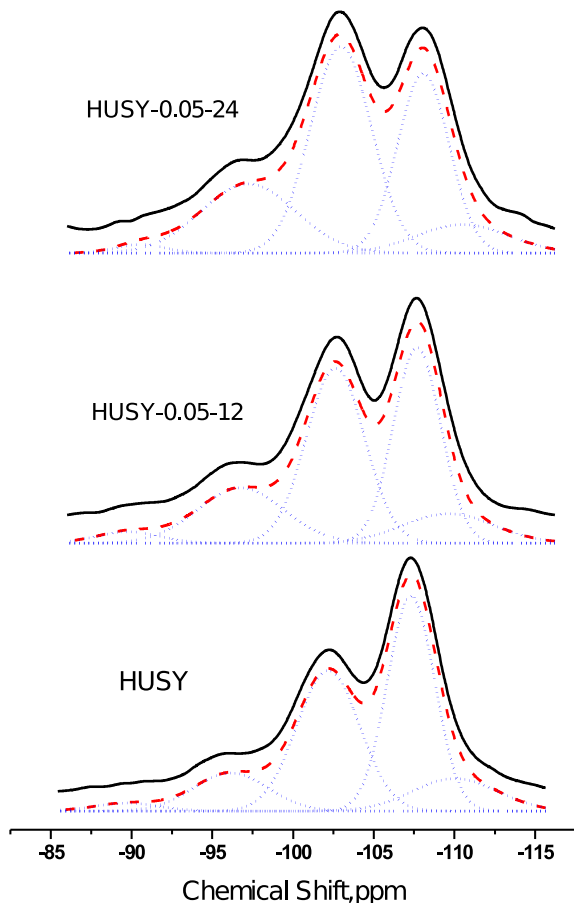


Fig. 2. Experimental and deconvoluted ^{29}Si MAS NMR spectra of HUSY, HUSY-0.05-12 and HUSY-24. Solid (—): experimental, dash (---): simulated, dot (···): deconvoluted.

150, 300 and 400 °C are listed in Table 3. It can be seen from the data that the number of Brønsted acid sites of aluminated HUSY is larger than that of the parent sample, and increases continuously with realumination. Comparing the change in the number of Lewis acid sites on HUSY zeolite before and after realumination, it can be stated that the number of weak acid sites on realuminated zeolites is lower than that on the parent zeolite, but the number of strong acid sites is significantly higher, showing the increase of the Lewis acid strength.

The acidity usually depends not only on the aluminum content in the framework and extra-framework of zeolite, but also on the coordination and distribution of the framework silicon and aluminium sites. The Si–OH–Al groups, including

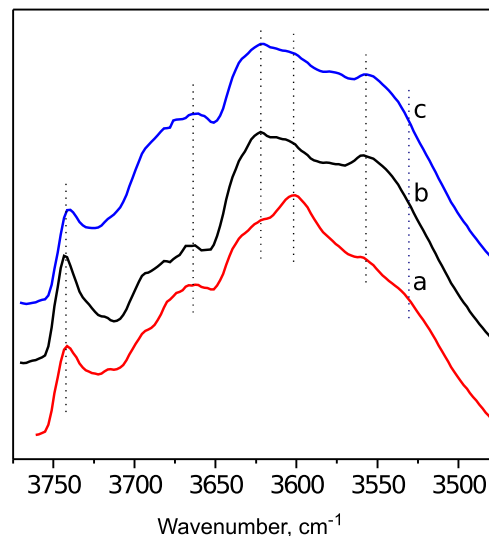


Fig. 3. FTIR spectra in hydroxyl region of a) HUSY, b) HUSY-0.05-12 and c) HUSY-0.05-24.

$\text{Si}_3\text{Si-OH-AlSi}_3$, $\text{AlSi}_2\text{Si-OH-AlSi}_3$, and $\text{Al}_2\text{SiSi-OH-AlSi}_3$ hydroxyls, correspond to the Brønsted acid sites, and Lewis acidity is generally associated with the presence of extra-framework Al species. According to ^{29}Si NMR and FTIR spectra of hydroxyl region, it is deduced that the increase in the contribution of Si(1Al) and Si(2Al) species on aluminated HUSY zeolites means the increase in the number of Brønsted acid sites. Otherwise, the decrease in the number of Lewis acid sites is accompanied by decreasing extra framework Al–OH.

3.3. Catalytic hydrogenation activity of HUSY supported Ru catalysts

The catalytic activity of Ru catalysts supported on HUSY zeolite before and after realumination in hydrogenation reaction of 0.5 wt.% benzene in hexane solution has been investigated. The conversion-time curves of three catalysts at the same reaction conditions are shown in Fig. 4. The experimental data of conversion (x) – time (t) were fitted according to the first-order kinetic equation:

$$\ln(1-x) = k_1 t \quad (1)$$

The kinetic rate constants ($k\sqrt{1}$) are 0.16, 0.84 and 0.88 h^{-1} for Ru/HUSY, Ru/HUSY-0.05-12 and Ru/HUSY-0.05-24, respectively. Compared with the parent HUSY supported catalyst, the catalysts on

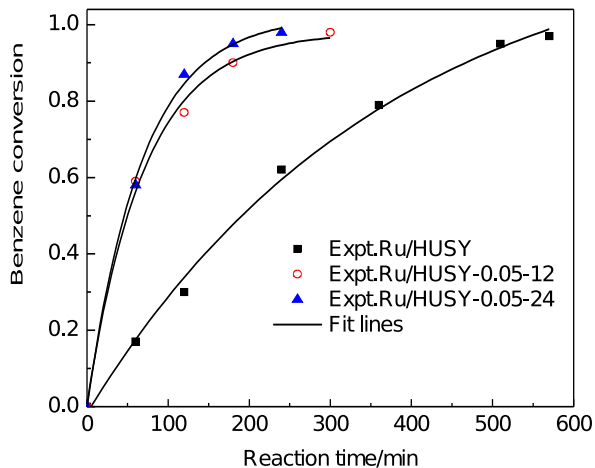


Fig. 4. Benzene hydrogenation on Ru/HUSY, Ru/HUSY-0.05-12 and Ru/HUSY-0.05-24.

aluminated supports display much higher hydrogenation rates, and the optimal activity is obtained for the most acidic Ru/HUSY-0.05-24 catalyst. It is well known that aromatics hydrogenation may occur on both metallic sites and acid sites close to the metal particles implying spillover of hydrogen from the metal surface or the metal-support boundary [11, 12]. The enhanced catalytic activity towards hydrogenation reactions on catalysts supported aluminated HUSY zeolites is related to higher surface area and acidity of support. The high surface area may increase the metal surface available for benzene conversion and the hydrogen dissociation on the metal, which increases hydrogen spillover. It is very important that increasing Brønsted acid sites in support enhances the active site concentration of the catalyst, resulting in an additional contribution to the overall hydrogenation rate of spillover hydrogen from the metal to the aromatic ring, adsorbed on the acid sites of the support.

4. Conclusion

HUSY zeolite was aluminated and mesostructured through a hydrothermal treatment with a dilute NaAlO₂ solution. A comprehensive characterization

by N₂ adsorption, XRD, FTIR spectroscopy and ²⁹Si MAS NMR revealed that the crystalline and pore structures of the HUSY zeolite were not been destroyed after realumination, and the realumination of zeolite occurred through isomorphous substitution of Si atom for Al atom on Si(0Al) sites, thus lowering Si/Al ratio of the zeolite framework. FTIR spectra of hydroxyl groups and adsorbed-pyridine showed an increased number of Brønsted acid sites after HUSY zeolites were realuminated. Accordingly, the Ru catalysts supported on aluminated HUSY zeolite displayed superior activity for benzene hydrogenation than those on the parent HUSY zeolite.

Acknowledgements

This work is supported by SinoPEC (No. 107009).

References

- [1] VAN DONK S., JANSSEN A.H., BITTER J.H., DE JONG K.P., *Catal. Rev.*, 45 (2003), 297.
- [2] BIAGLOW A.I., PARRILLO D.J., KOKOTAILO G.T., GORTE R.J., *J. Catal.*, 148 (1994), 213.
- [3] FRITZ P.O., LUNSFORD J.H., *J. Catal.*, 118 (1989), 85.
- [4] WANG Q.L., GIANNETTO G., GUISNET M., *J. Catal.*, 130 (1991), 471.
- [5] YANG C., WANG J., XU Q., *Micropor Mater.*, 11 (1997), 261.
- [6] MA J., MA N., XUE ZH., WANG Y., LI R., *Stud. Surf. Sci. Catal.*, 174 (2008), 257.
- [7] DATKA J., SULIKOWSKI B., GIL B., *J. Phys. Chem.*, 100 (1996), 11242.
- [8] SULIKOWSKI B., DATKA J., GIL B., PTASZYNSKI J., KLINOWSKI J., *J. Phys. Chem. B*, 101 (1997), 6929.
- [9] CAICEDO-REALPE R., PÉREZ-RAMÍREZ J., *Micropor. Mesopor. Mat.*, 128 (2010), 91.
- [10] XU B., BORDIGA S., PRINS R., VAN BOKHOVEN J.A., *Appl. Catal. A*, 333 (2007), 245.
- [11] LIN S.D., VANNICE M.A., *J. Catal.*, 143 (1993), 563.
- [12] SIMON L.J., VAN OMMEN J.G., JENTYS A., LERCHER J.A., *Catal. Today*, 73 (2002), 105.

Received: 2011-08-12

Accepted: 2012-11-05